

# A GMCSF and IL-15 fusokine leads to paradoxical immunosuppression in vivo via asymmetrical JAK/STAT signaling through the IL-15 receptor complex

Mouth Rafei,<sup>1</sup> Jian Hui Wu,<sup>2</sup> Borhane Annabi,<sup>3</sup> Laurence Lejeune,<sup>1</sup> Moïra François,<sup>1</sup> and Jacques Galipeau<sup>1,4</sup>

<sup>1</sup>The Montreal Centre for Experimental Therapeutics in Cancer, Jewish General Hospital, McGill University, Montreal, QC, <sup>2</sup>Molecular Oncology Laboratory, McGill University, Montreal, QC; <sup>3</sup>Department of Chemistry, University of Quebec at Montreal (UQAM), Montreal, QC; and <sup>4</sup>Division of Hematology/Oncology, Jewish General Hospital, McGill University, Montreal, QC

**We hypothesized that a granulocyte macrophage colony-stimulating factor (GMCSF) and interleukin 15 (IL-15) fusokine (GIFT15) would possess greater immunostimulatory properties than their combined use. Unexpectedly, tumor cells engineered to secrete GIFT15 protein led to suppression of natural killer (NK) and NKT-cell recruitment in vivo, suggesting an unanticipated immune-suppressive effect. We found GIFT15 to have pleiotropic effects on an array of immune-competent cells. Among these, macrophages treated with GIFT15 secrete de novo the tissue**

**inhibitor of metalloproteinase-2 (TIMP-2); activated matrix metalloproteinase-2 (MMP-2); transforming growth factor- $\beta$  (TGF- $\beta$ ); as well as vascular endothelial growth factor (VEGF). We show that the GIFT15 fusokine has increased affinity for the  $\alpha$  chain component of the IL-15R, leading to aberrant signaling through the  $\beta$  chain manifested by the hyperphosphorylation of STAT3 both in macrophages and splenocytes. Suppression of common  $\gamma$  chain-mediated STAT5 phosphorylation and blockade of the IL-15-dependent IFN- $\gamma$  response in mouse splenocytes**

**were also observed. We tested GIFT15 as an immunosuppressor and demonstrated that it allowed engraftment of allogeneic B16F0 and human xenograft U87GM glioma cells in immunocompetent mice. Thus, GIFT15 defines a new class of fusokine that mediates proangiogenic and immunosuppressive effects via aberrant signaling by the IL-15R in lymphomyeloid cells. (Blood. 2007;109:2234-2242)**

© 2007 by The American Society of Hematology

## Introduction

Immune-stimulatory cytokines can be exploited to treat human ailments including cancer. Among the cytokines identified for such use, GMCSF has been under much scrutiny due to its direct action on the adaptive immune system through the enhancement of antigen presentation as well as costimulation.<sup>1,2</sup> Furthermore, second-generation strategies linking innate and adaptive immunity using GMCSF delivered as a fusion cytokine (fusokine) with other immune-stimulatory proteins such as IL-2 are currently being developed.<sup>3,4</sup> The utility of GMCSF-containing fusokines having been established in animal models of cancer immunotherapy begets the testing of novel combinatorial fusokines, especially since the biochemical behavior of such chimeras can lead to unprecedented biopharmaceutical properties as we have previously reported.<sup>4</sup> IL-15 possesses overlapping activities with IL-2 such as the activation of T cells and the stimulation of natural killing<sup>5</sup> as well as additive stimulatory effects on the immune system distinct from IL-2.<sup>6,7</sup> These features make IL-15 an attractive companion to GMCSF as part of an immunotherapeutic fusokine. In fact, it was previously reported that cotreatment of dendritic cell (DC) precursors with GMCSF and IL-15 as separate entities can generate a powerful T-helper 1 (Th1) immune response both in vitro and in vivo.<sup>8</sup> Thus, we hypothesized that the generation of a GMCSF and IL-15 fusion transgene (hereafter GIFT15) would lead to immunostimulatory synergy in the setting of cancer immunotherapy. Unexpectedly, we found that the GIFT15 fusokine behaved in a manner opposite to what was anticipated and possessed profoundly immune-suppressive properties as well as robust proangiogenic features in vivo. These unanticipated features were found

to arise from asymmetrical JAK/STAT signaling through the IL-15 receptor complex in responsive lymphomyeloid cells. This novel pharmaceutical effect was further characterized in the setting of allogeneic and xenogeneic somatic cell transplantation. Here we describe our findings that support the potential use of GIFT15 as a novel immunosuppressive compound.

## Materials and methods

### Animals, cell lines, recombinant proteins, antibodies, and ELISA kits

All experimental mice were females aged 6 to 8 weeks (Jackson Laboratory, Bar Harbor, ME). The C57Bl/6-derived B16F0 and human U87GM cell lines were cultured in DMEM (Wisent Technologies, Rocklin, CA) supplemented with 10% FBS (Wisent Technologies) and 50 U/mL Pen/Strep (Wisent Technologies). The cell lines JAWSII and CTLL2 (American Type Culture Collections [ATCC], Manassas, VA) were grown according to ATCC's recommendations. Biochemical reagents used were as follows: recombinant proteins (rIL-15/rIL-15R $\alpha$ -Fc/rGMCSF/rTGF- $\beta$ /rMMP2/rMMP9) and their antibodies (R&D Systems, Minneapolis, MN); anti-TIMP2 polyclonal antibodies and rTIMP2 (Chemicon, Temecula, CA); antibodies against VWF (von Willebrand factor) and  $\alpha$ -tubulin (Santa Cruz Biotechnology, Santa Cruz, CA); polyclonal antiphosphorylated STAT3, and phosphorylated STAT5, STAT3, STAT5, or Bcl-XL (Cell Signalling Technology, Danvers, MA); anti-mouse FcR III/II, CD3, CD4, CD8, NK1.1, IFN- $\gamma$ , or isotype control antibodies for flow cytometry (BD

Submitted July 25, 2006; accepted October 17, 2006. Prepublished online as *Blood* First Edition Paper, November 2, 2006; DOI 10.1182/blood-2006-07-037473.

The online version of this article contains a data supplement.

The publication costs of this article were defrayed in part by page charge payment. Therefore, and solely to indicate this fact, this article is hereby marked "advertisement" in accordance with 18 USC section 1734.

© 2007 by The American Society of Hematology

Biosciences, San Diego, CA); enzyme-linked immunosorbent assay (ELISA) kits for mVEGF, mL-15 (R&D Systems), or mIFN- $\gamma$  (BD Biosciences); angiogenic protein arrays (Panomics, Fremont, CA); and Multiscreen-MIC plates (Millipore, Cambridge, ON).

### Vector construct and protein modeling

The mouse IL-15 cDNA (Invivogen, San Diego, CA) was modified to remove the 3' nucleotides encoding the STOP codon and subsequently cloned in frame with the cDNA encoding mouse GMCSF cDNA to generate the cDNA for GIFT15 fusokine. The GIFT15 cDNA was incorporated into a bicistronic retrovector allowing the expression of both the fusokine and GFP reporter.<sup>4</sup> To build a structural model of GIFT15 by homology modeling, crystal structures of human GMCSF (accession code 2gmf) and human IL-2 (D chain, accession 1erj) were used as templates for mouse GMCSF and mouse IL-15, respectively. The structural template for the region connecting GMCSF and IL-15 (accession code 1orc) was identified by fold recognition methods, using software PROSPECT v2 (Oak Ridge National Laboratory, Oak Ridge, TN). Based on the templates identified, 50 structural models of GIFT15 were generated using software MODELLER v6 (University of California at San Francisco). A structural model of GIFT15 in complex with cytokine receptor was generated based on the crystal structure of the IL-2 signaling complex (accession 1erj), which is the trimeric assembly of IL-2R $\alpha$ , IL-2R $\beta$ , and IL-2R $\gamma$  in complex with IL-2.

### Fusokine expression and functional assays

Infectious retroviruses encoding GIFT15 were generated with 293-GP2 packaging cell (Clontech, Mountain View, CA) and concentrated retroviruses were used to gene modify B16F0 melanoma and U87 glioma cells. To test the bioactivity of GIFT15, the IL-2-responsive CTLL-2 or GMCSF-responsive JAWSII cell lines were plated at a density of  $10^5$  cells/well in a 96-well plate and treated with increasing concentrations of cytokines for 72 hours. Cell proliferation was assessed with a 3-(4,5-dimethylthiazol-2-yl)-2,5-diphenyltetrazolium bromide (MTT) assay.

### Murine B16F0 tumor implantation in syngeneic C57Bl/6 mice and immune infiltrate analysis

One million cytokine-secreting B16F0 cells were injected subcutaneously in C57Bl/6 mice, and tumor growth was monitored over time. All implanted B16F0 polyclonal populations produced comparable molar quantities of cytokines ( $0.6 \pm 0.1$  pmol/ $10^6$  cells/24 hours). For immune infiltrate analysis, one million cytokine-secreting B16F0 cells were mixed with 500  $\mu$ L Matrigel (BD Biosciences) at 4°C and injected subcutaneously in C57Bl/6 mice. Implants were surgically removed 2 weeks after transplantation and digested as reported previously.<sup>4</sup> After incubation with anti-FcR III/II mAb for 1 hour, cells were incubated for 1 hour at 4°C with appropriate antibodies and analyzed by flow cytometry using a Becton Dickinson FACScan (San Jose, CA).

### Murine B16F0 tumor implantation in NOD-SCID mice

One million GIFT15-secreting or GFP-expressing B16F0 cells were injected subcutaneously in immunocompromised nonobese diabetic-severe combined immunodeficient (NOD-SCID) mice, and tumor growth was monitored over time. For *VWF* immunostaining, animals were killed and tumors retrieved for paraffin embedment before being cut and probed with anti-*VWF* as reported elsewhere.<sup>9</sup> Total blood vessels were counted and divided by the total surface area calculated using Scion image software (Scion, Frederick, MD) to obtain blood vessel density.

### Macrophage migration assays, intracellular signaling, and cytokine secretion

Peritoneal macrophages were isolated from C57Bl/6 mice by peritoneal lavage and used for all macrophage-based *in vitro* assays. For migration assays,  $10^5$  macrophages per well were plated in the top chambers of a Transwell plate and the lower chambers were filled, in triplicate with 500  $\mu$ L serum-free RPMI to which conditioned media (CM) derived from

cytokine-expressing B16 cells were added to achieve a final cytokine concentration of 0.1 or 1 nM. After 18 hours of incubation at 37°C, the cells on the bottom filter of each well were counted at 10 high-power fields ( $\times 400$ ). For signaling analysis, GIFT15 was purified using an immunoaffinity column packed using CNBr-sepharose (Amersham, Piscataway, NJ) according to the manufacturer's instructions and 30 pmol purified cytokines were added to  $10^6$  macrophages for 15 minutes before being lysed and probed by Western blot (WB) with rabbit antiphosphorylated STAT3 or STAT5. Total STAT3 or STAT5 proteins were used as loading controls. For analysis of macrophage secretome, macrophages were cultured with 30 pmol cytokines for 72 hours at 37°C, and supernatants screened using angiogenic protein arrays and ELISA according to the manufacturer's instructions.

### Surface plasmon resonance (SPR)

The binding interaction between GIFT15 and the IL-15 receptor  $\alpha$  chain was examined in real-time using a BIACORE 3000 with research-grade CM5 sensor chips (Biacore AB, Uppsala, Sweden) prepared by immobilizing purified recombinant IL-15R $\alpha$ -Fc fusion protein (R&D Systems) at a concentration of 10  $\mu$ g/mL in 10 mM sodium acetate, pH 5.0, using the Amine Coupling Kit (Biacore AB) and HBS-M running buffer. Corresponding reference surfaces were prepared in a similar manner in the absence of any ligand addition. As a positive control, rIL-15 was injected at 50  $\mu$ L/min (180-second association + 180-second dissociation) over the reference and amine-coupled rIL-15R $\alpha$ -Fc surfaces (1300 RU). Regeneration was achieved using 2 30-second pulses of HBS-M containing 0.5 M NaCl, 50 mM EDTA, and 0.05% (vol/vol) TritonX-100. For the test sample, purified GIFT15 was injected over the same sensor chip surfaces and regenerated in an identical manner. All binding data presented were "double-referenced" and analyzed according to a 1:1 interaction model using BIAevaluation 4.1 (Biacore AB).

### GIFT15-mediated biochemical responses in splenocytes

Splenocytes were collected from normal C57Bl/6 mice. Media containing 30 pmol cytokines were used to stimulate  $10^6$  splenocytes for 15 minutes and cell lysates generated for Western blot analysis with antiphosphorylated STAT3, STAT5, and Bcl-XL. For apoptosis assays,  $10^6$  splenocytes were cultured using the same conditions for 36 hours and then stained with propidium iodide (PI) and for annexin-V. For splenocyte proliferation assays,  $10^5$  splenocytes were cultured with increasing concentrations of cytokines for 72 hours at 37°C and compared by MTT assay. To assess IFN- $\gamma$  secretion generated as part of a 2-way mixed lymphocyte reaction (MLR), the supernatant of  $10^5$  splenocytes stimulated for 36 hours with equimolar concentrations of cytokines was centrifuged and used to detect IFN- $\gamma$  secretion by ELISA. For the MLR assay,  $1.5 \times 10^5$  splenocytes from normal BALB/c and C57Bl/6 mice were mixed or treated separately with GIFT15. All cells were incubated at 37°C for a period of 72 hours and then IFN- $\gamma$  tested by ELISA. Intracellular IFN- $\gamma$  staining on mouse splenocytes was performed using the BD Cytotfix/Cytoperm Kit (BD Biosciences).

### Allogeneic B16F0 and xenogenic U87GM tumor implantation

Allogeneic tumor cell implantation was performed by injecting  $10^7$  live B16-GFP or B16-GIFT15 in BALB/c mice and tumor growth followed over time. For spleen analysis, animals with GIFT15 tumors exceeding 1000 mm<sup>3</sup> or with the largest B16-GFP tumors were killed and the spleen was removed and weighed. Paraffin-embedded slides were also prepared for hematoxylin and eosin (H&E) staining and visualized using a Zeiss Axiovert 25 microscope (Carl Zeiss, Toronto, ON, Canada) with a  $40\times 0.55$  NA objective. Pictures were taken using a Sony VX-DSC-W5 Mpegmovie digital camera (Sony, Tokyo, Japan). For flow cytometry analysis, splenocytes were stained and analyzed by fluorescence-activated cell sorting (FACS). For xenogenic tumor cell implantation,  $10^7$  live human U87-GFP or U87-GIFT15 transduced tumor glioma cells were implanted subcutaneously. Tumor growth and graft survival were monitored over time in wild-type C57Bl/6, CD4<sup>-/-</sup>, CD8<sup>-/-</sup>, or beige (natural killer [NK] deficient) mice.

## Statistical analysis

*P* values were calculated using the paired Student *t* test.

## Results

### Design and characterization of murine GIFT15

The fusokine was created by cloning a modified GMCSF cDNA missing the nucleotides coding for the last 11 carboxy-terminal amino acids (aa's), in frame with the 5' end of the mouse IL-15 cDNA, including its long signal peptide.<sup>6,7</sup> The final fusokine GIFT15 cDNA encodes for a single polypeptide chain of 299 aa's (Figure 1A). Computer-based analysis of the 3-dimensional structure revealed that the 7-aa peptidic bridge and the uncleaved IL-15 long signal peptide sequence form an intercytokine bridge of 55 aa's in length with a 3 alpha helix configuration (Figure 1B). Denaturing immunoblotting performed on the supernatant from B16F0 cells retrovirally transduced to express GIFT15 showed that the chimeric protein was efficiently secreted into the extracellular space and migrated at a molecular weight of 55 kDa (Figure 1C). The bioactivity of both cytokine subunits within GIFT15 was confirmed by the proliferation of the GMCSF-dependent JAWSII and IL-15-dependent CTLL2 cell lines, respectively (Figure 1D).

### GIFT15 promotes tumor growth by blocking the recruitment of NK/NKT cells and by inducing angiogenesis

To assess the ability of GIFT15 to induce an immune modulatory effect, polyclonal populations of B16F0 cells engineered to secrete equimolar levels of cytokines were injected subcutaneously in syngeneic immune-competent C57Bl/6 mice. We observed that B16F0 cells secreting GIFT15 (hereafter B16-GIFT15) had ac-

quired aggressive growth properties with an average tumor size 3-fold larger than that of control groups in the weeks following implantation (Figure 2A). To determine whether this phenomenon was linked to an atypical immune response, we analyzed tumor infiltration by immune cells 2 weeks after implantation of Matrigel matrix embedded cells. We found that NK and NKT cells were virtually absent in GIFT15-secreting tumors when compared with B16-GMCSF or B16-IL-15 control groups, while the number of other CD3<sup>+</sup> T-cell subsets was similar to controls (Figure 2B). The observed absence in NK/NKT-cell recruitment by B16-GIFT15 cells contradicted what we predicted would occur in vivo, especially since IL-15 has been shown by others to directly stimulate the development, expansion, recruitment, and activation of NK and NKT cells.<sup>10-13</sup> B16-GIFT15 cells implanted in immunocompromised NOD-SCID mice also showed significantly enhanced tumorigenicity where we would have predicted a similar tumor growth rate to controls if immunosuppression was solely at play (Figure 2C). Histologic analysis of explanted tumors by immunostaining against *VWF* revealed a 3-fold increase in blood vessel density ( $P < .05$ ) in B16-GIFT15 tumors compared with the control (Figure 2D) as well as a robust 4-fold increase of infiltration by tumor-associated macrophages (TAMs) (data not shown).

### GIFT15 effect on macrophages

TAMs play an important role in immunosuppression and angiogenesis.<sup>14-16</sup> The GIFT15-secreting tumors showed a 4-fold increase in macrophage content when compared with control B16 tumors (data not shown), suggesting a powerful macrophage chemotactic property for the fusokine in vivo. Macrophages are known to express the IL-15 receptor (IL-15R) where intracellular signaling occurs through the  $\beta$  chain (JAK1/STAT3)

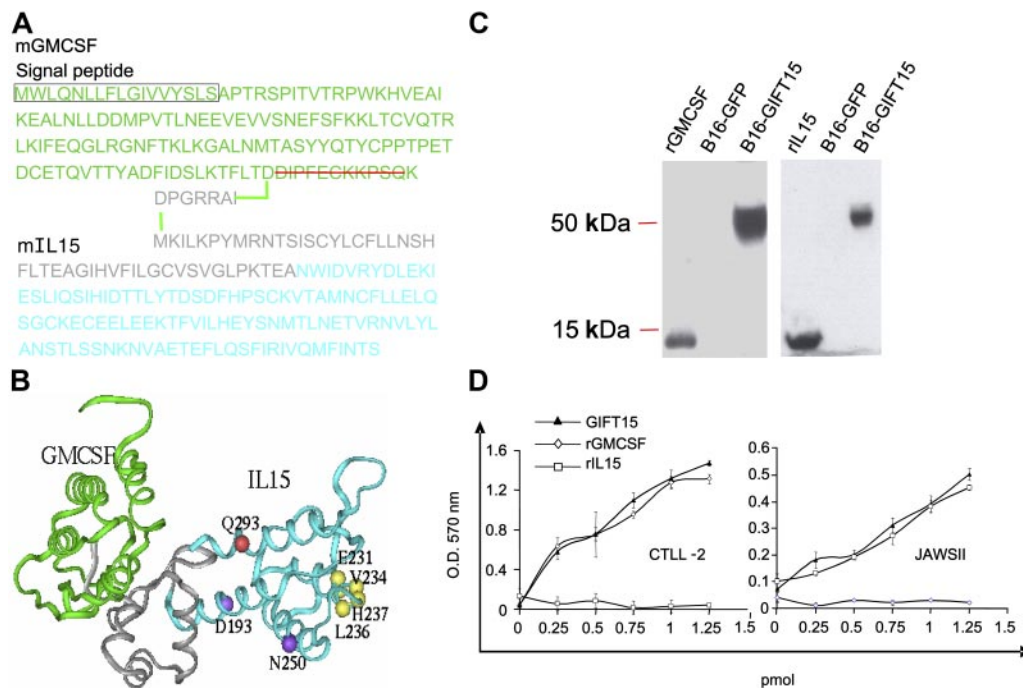
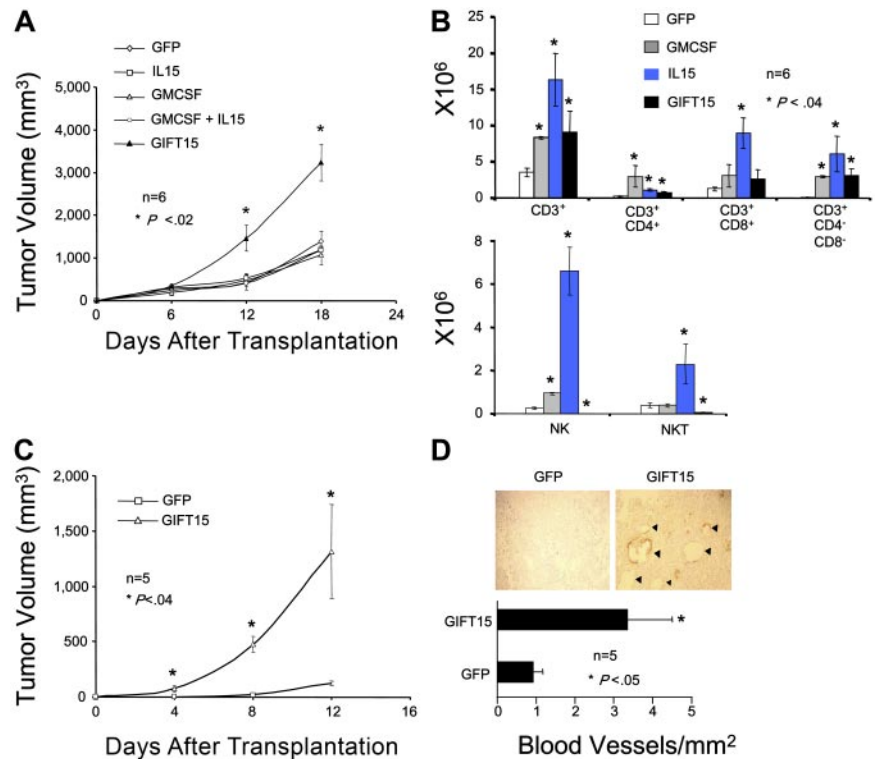


**Figure 1. Design and expression of GIFT15 fusokine.** (A) Schematic representation of the GIFT15 aa sequence. (B) The predicted structural model of GIFT15. GMCSF is shown in green ribbon; intercytokine bridge, in gray ribbon; and IL-15, in cyan ribbon. The IL-15 residues experimentally identified to interact with IL-15R $\alpha$ , IL-2R $\beta$ , and IL-2R $\gamma$  are shown by yellow, purple, and red balls, respectively. (C) Denaturing immunoblot using conditioned media (CM) from genetically-modified B16F0 expressing the green fluorescent protein (GFP) or GIFT15 probed with polyclonal goat anti-IL-15 or anti-GMCSF antibodies. rIL-15 and rGMCSF were used as positive controls. (D) Biologic activity of GIFT15. To test the bioactivity of GIFT15, proliferation assays were performed by MTT incorporation using CTLL-2 and JAWSII cell line concentrations (CTLL-2,  $P > .05$  between GIFT15 and IL-15; JAWSII,  $P > .05$  between GIFT15 and GMCSF). Results are shown as mean of triplicates  $\pm$  SEM of 1 representative experiment of 3.

**Figure 2. GIFT15 possesses NK/NKT depleting and proangiogenic properties.** (A) GIFT15 effect on tumor growth in syngeneic immunocompetent C57Bl/6 mice. C57Bl/6 mice ( $n = 6$ ) were injected with  $10^6$  live cytokine-secreting B16F0 cells and tumor volume was monitored over time ( $P < .05$  between B16-GIFT15 and B16-GFP/IL-15/GMCSF/IL-15 + GMCSF). Results are shown as mean tumor volume  $\pm$  standard error of the mean (SEM). (B) Immune infiltrate analysis. Single cell suspensions were generated from the enzymatic dissociation of matrix embedded B16F0 cells retrieved from mice that were killed 2 weeks after transplantation and analyzed by flow cytometry ( $P < .04$  between experimental groups and B16-GFP). Results are shown as mean of 6 replicates  $\pm$  SED. (C) GIFT15 effect on tumor growth in NOD-SCID mice. NOD-SCID mice ( $n = 5$ ) were injected with  $10^6$  live B16-GFP or GIFT15 cells, and tumor volume was assessed over time ( $P < .02$  between B16-GIFT15 and B16-GFP). Results are shown as mean tumor volume  $\pm$  SED. (D) Blood vessel density in tumors grown in NOD-SCID mice. Tumors removed from NOD-SCID mice that had been killed ( $n = 5$ ) were paraffin-embedded, prepared on slides, and then stained against VWF. Blood vessel density was calculated by dividing total amount of blood vessels by the tumor's surface area ( $\text{mm}^2$ ) ( $P < .05$  between B16-GIFT15 and B16-GFP). Results are shown as mean blood vessel density  $\pm$  SED.



and the  $\gamma$  chain (JAK3/STAT5). We therefore tested the chemotactic properties of GIFT15 on mouse peritoneal macrophages to further define IL-15R-mediated signaling pathways *in vitro*. The chemotactic effect of 0.1 nM GIFT15 on macrophages was significantly greater than that of control cytokines at equal or higher (1 nM) concentrations (Figure 3A), confirming the hypothesis that GIFT15 has the potential to enhance locoregional recruitment of TAMs as observed *in vivo*. On a molecular level, IL-15R-mediated signaling analysis showed that STAT3 was hyperphosphorylated in response to GIFT15 when compared with control groups, whereas STAT5 activation was similar to the response induced by rIL-15 (Figure 3B). Stimulation of macrophages using rIL-15 and rGMCSF led to an additive effect on STAT5 phosphorylation, whereas the fusokine containing both moieties failed in generating the same level of phosphorylation (Figure 3B). To better understand the cell physiological consequences of asymmetrical signaling on macrophages at a cellular level, conditioned media (CM) from cytokine treated macrophages were probed using a commercial angiogenic protein array, revealing the presence of TIMP-2 following GIFT15 exposure, which was then confirmed by Western blot (Figure 3C). Since TIMP-2 is implicated in the activation of MMP-2,<sup>17</sup> CM from treated macrophages were assayed by gelatin zymography. As shown in Figure 3D, the GIFT15-treated group led to MMP-2 activation as determined by gelatin degradation. MMP-2 was also detected at the protein level by WB, confirming the data obtained by zymography, whereas MMP-9 was totally absent (Figure 3E). Since peritoneal macrophages stimulated with GIFT15 led to the activation of MMP-2, and the latter is known to play a role in angiogenesis,<sup>17-19</sup> we were interested in identifying additional macrophage-derived molecules that might help explain the increased blood vessel density observed *in vivo*. In comparison with control groups, GIFT15 treatment of macrophages leads to significant secretion/activation of TGF- $\beta$  (Figure 3F) and VEGF (Figure

3G). Taken together, these data suggest that GIFT15-stimulated macrophages likely contribute to the observed *in vivo* immunosuppression via TGF- $\beta$  production in addition to angiogenesis through MMP-2 and VEGF secretion and activation.

#### GIFT15 leads to hyperphosphorylation of STAT3 and blockade of STAT5 activation in lymphoid cells

CD3<sup>+</sup> and NK/NKT lymphoid cells express the full IL-15R composed of the  $\alpha$ ,  $\beta$ , and common  $\gamma$  chains.<sup>5-7</sup> In order to further characterize the molecular mechanism by which GIFT15 exerts its suppressive effects on lymphoid cells, we first assessed the interaction of GIFT15 with individual components of the IL-15R.<sup>6,7</sup> Although the  $\beta$  and  $\gamma$  chains of the IL-15R are components shared by the IL-2R complex, the high-affinity IL-15R $\alpha$  chain provides specificity. Its binding affinity to GIFT15 was assessed by BIAcore analysis. We found that the average dissociation equilibrium ( $K_d$ ) of rIL-15 was of 3 nM, whereas purified GIFT15 interacted with a higher affinity with an average  $K_d$  of 1.4 nM (Figure 4A). Since IL-15R-dependent intracellular signaling in immune-competent cells occurs through JAK/STAT downstream of both the  $\beta$  chain and the  $\gamma$  chain, we investigated the effect of GIFT15 on these pathways in primary mouse splenocytes. After 15 minutes of stimulation with GIFT15 or controls in equimolar concentrations, we found that the fusion protein substantially increased the  $\beta$  chain-dependent phosphorylation of STAT3 and suppressed the  $\gamma$  chain-dependent phosphorylation of STAT5 (Figure 4B). To determine the effect of GIFT15 on GMCSF receptor complex (GMCSFR)-mediated signaling, we examined STAT5 phosphorylation following stimulation of JAWS-II cells, a GMCSF-dependent cell line devoid of the IL-15R. We did not observe any difference between GMCSF- and GIFT15-mediated activation of STAT5 in this cell line, suggesting that GIFT15 binds to and activates the GMCSFR in a manner indistinguishable from that of monomeric GMCSF (Figure 4C). This observation suggests

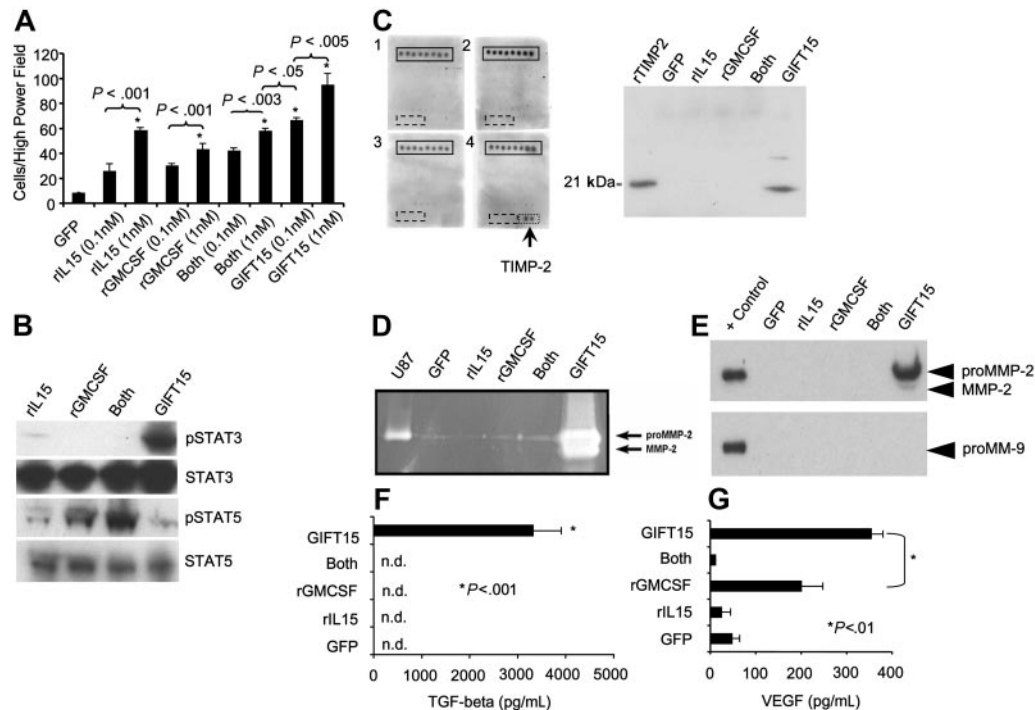


**Figure 3. Peritoneal macrophage responses following GIFT15 treatment.** (A) In vitro macrophage migration assay. Peritoneal macrophages were plated for 18 hours in transwell plates with lower chambers filled in triplicate with cytokines at increasing molarities. The cells on the bottom filters of 10 high-power fields ( $\times 400$ ) were counted for each well, and the results are depicted as mean cell number per high-power field  $\pm$  SED. (B) STAT3/STAT5 phosphorylation in peritoneal macrophages. Macrophages ( $10^6$ ) were stimulated for 15 minutes with 30 pmol rIL-15, rGMCSF, or both cytokines inoculated in B16-GFP CM or with B16-GIFT15 CM, and cell lysate was probed for phosphorylated STAT3/STAT5. Total STAT3 or STAT5 protein was used as loading control. (C) TIMP-2 secretion from GIFT15-treated macrophages. Peritoneal macrophages treated with 30 pmol cytokines in serum-free media were incubated for 72 hours and media tested by angiogenic protein arrays (U87 supernatant was used as positive control). TIMP-2 detection was further confirmed by WB (+ control is either rMMP2 or rMMP9). (D) GIFT15 treatment induces the secretion and activation of MMP2. Macrophages ( $10^6$ ) were deprived of serum and cultured with 30 pmol cytokines. Gelatin zymography was performed, and the hydrolytic activity of MMP-2 was assessed. (E) A confirmation by WB was performed to verify that MMP-2 but not MMP-9 was indeed induced by GIFT15. (F) Macrophage treatments with GIFT15 induce active TGF- $\beta$ . Serum-free supernatant collected from macrophages treated with 30 pmol cytokines was assessed for the presence of active TGF- $\beta$ , and only the GIFT15 group led to its detection. (G) GIFT15-treated macrophages led to VEGF secretion. Stimulated peritoneal macrophages treated as previously mentioned were assessed by ELISA for the secretion of VEGF. Even though GMCSF led to modest secretion of VEGF, the GIFT15-treated group had a higher concentration than the remaining groups. Results are shown as mean  $\pm$  SED ( $n = 3$ ).

that the function of the GMCSF moiety of GIFT15 remains unchanged despite the tethering of IL-15 at its carboxy-terminus. The asymmetrical signaling through the IL-15R mediated by GIFT15 suggests that an altered ligand/receptor interaction is at play. As a hypothesis-generating experiment, we used molecular modeling to predict GIFT15 and IL-15R interaction at the structural level. Based on the known molecular structure of IL-15 interaction with the IL-15R $\alpha$  chain<sup>20,21</sup> and on the predicted homologous interaction of IL-15 with the IL-15R $\beta$  and  $\gamma$  chains to that of IL-2,<sup>22</sup> we modeled the best fit for GIFT15 with the IL-15R (Figure 4D). This virtual interaction suggests that the GMCSF domain component of the GIFT15 fusokine may hinder the interaction of the IL-15 domain component with the IL-15R $\gamma$  chain, explaining in part the observed down-regulation of signaling through the JAK3/STAT5 pathway.

#### GIFT15 protects splenocytes from apoptosis, stimulates proliferation, and blocks IFN- $\gamma$ secretion

STAT3 activation has been linked to a variety of biochemical and cellular events such as survival, proliferation, angiogenesis, and immunosuppression.<sup>23-26</sup> Since we have shown that splenocytes hyperphosphorylate STAT3 in response to GIFT15, we tested whether GIFT15 enhances survival of splenocytes in vitro using serum-free media as a proapoptotic stimulus. Splenocytes stained for PI and annexin-V revealed that 83% of cells treated with GIFT15 survived compared with 33% with rGMCSF, 43% using rIL-15, or 41% with both molecules (Figure 5A). In addition, cell

lysate immunoblotting against the antiapoptotic molecule Bcl-XL (Figure 5A) provided evidence that GIFT15 rescues splenocytes from cell death through an increase in Bcl-XL level, a process known to occur when STAT3 is dominantly activated.<sup>23,24</sup> Of interest, splenocyte proliferation does not seem to be affected by the relative decrease in STAT5 phosphorylation (Figure 5B;  $P < .05$ ) despite the fact that the latter is associated with mitogenic activities.<sup>27-29</sup> Based on the asymmetrical signaling mediated by GIFT15 through the IL-15R, we tested for expression levels of known target genes of STAT5 in immune-competent cells—such as IFN $\gamma$ <sup>7</sup>—which may help to explain the observed immunosuppressive effects in vivo. Although GIFT15-treated splenocytes proliferate normally when compared with rIL-15, the IFN- $\gamma$  response was completely abrogated when the fusokine was added to the system as opposed to a strong induction with rIL-15 alone or in the presence of rGMCSF (Figure 5C,  $P < .001$ ).

#### GIFT15 can block lymphocyte activation arising from a mixed lymphocyte reaction and allows engraftment of GIFT15-expressing allogeneic somatic cells in immune-competent recipients

Since GIFT15 can signal aberrantly through the IL-15R by hyperphosphorylating STAT3 without leading to IFN- $\gamma$  secretion in lymphocytes, we wanted to test its ability to inhibit IFN- $\gamma$  secretion in a 2-way MLR between MHC-mismatched C57Bl/6 and BALB/c splenocytes and found that 0.18 pmol purified GIFT15 was enough to suppress IFN- $\gamma$  secretion levels by 6-fold (Figure 6A). We

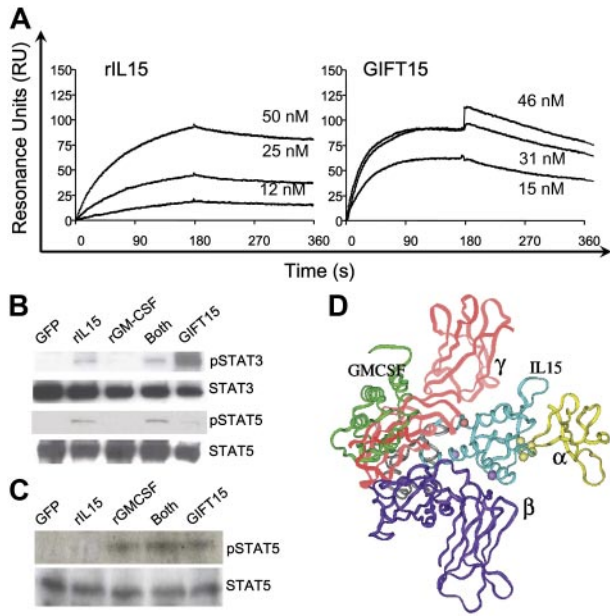


**Figure 4. GIFT15 and receptor-mediated signaling.** (A) BIAcore analysis of IL-15R $\alpha$  chain interaction with rIL-15 and purified GIFT15. Representative sensorgrams for the binding of (A) 12, 25, or 50 nM rIL-15 or (B) 15, 31, or 46 nM purified GIFT15 to 1300 RU IL-15R $\alpha$ -Fc as detected by SPR. (B) GIFT15-induced phosphorylation of STAT3/5 protein. Splenocytes ( $10^6$ ) were stimulated for 15 minutes with 30 pmol rIL-15, rGM-CSF, or both cytokines inoculated in B16-GFP CM or with B16-GIFT15 CM, and cell lysate was probed for phosphorylated STAT3/STAT5. Total STAT3 or STAT5 protein was used as loading control. GIFT15-induced phosphorylation of STAT5 protein. (C) GM-CSFR-mediated signaling. JAWS-II cells ( $10^6$ ) were stimulated as performed previously with primary splenocytes, and cell lysate was probed for phosphorylated STAT5. Total STAT5 protein was used as loading control. (D) Structural model of GIFT15 (green, gray, and cyan ribbon) complexed with IL-15R $\alpha$  (yellow ribbon), IL-2 $\beta$  (purple ribbon), and IL-2R $\gamma$  (red ribbon).

examined IFN- $\gamma$  production by intracellular staining in T cells as part of the 2-way MLR and found that GIFT15 abolished IFN- $\gamma$  production by CD3/CD4 and CD3/CD8 T cells (Figure S1, available on the *Blood* website; see the Supplemental Figure link at the top of the online article). This observation implies that the fusokine may be exploited for tolerance induction to allogeneic cells. To test this hypothesis,  $10^7$  B16-GFP or B16-GIFT15 cells were injected subcutaneously in MHC-mismatched BALB/c mice, and tumor growth was assessed as a measure of graft tolerance. Even though the B16-GFP graft was rejected completely 2 months after transplantation, the B16-GIFT15 cells led to continuous tumor growth up to a volume of 1000 mm<sup>3</sup> (Figure 6B). BALB/c mice with established B16-GIFT15 tumors were killed and their spleens collected for analysis. The spleens of control mice had normal white pulp structures. In contrast, spleens from GIFT15 mice had a loss of distinguishable white and red pulps (Figure 6C). In addition, spleens from the GIFT15 group were enlarged, suggesting that splenocytes proliferate in vivo in response to GIFT15 secreted from the B16-GIFT15 tumors (Figure 6C). Although the number of splenocytes increased, there was no apparent selective expansion of a lymphoid subset in the GIFT15 group (Figure 6D).

**GIFT15 allows for xenotransplantation of the human glioma U87GM in immunocompetent mice**

We tested the limits of GIFT15-mediated tolerance in the context of xenotransplantation using the human glioma cell line U87GM transduced to secrete the GIFT15 fusokine. GIFT15-secreting tumors were accepted in all mice until day 224, at which time half of the group rejected the graft. All control mice had rejected the

U87-GFP graft 12 days after transplantation (Figure 7A-B). However, wild-type C57Bl/6 mice allowed the GIFT15-secreting tumor graft to survive for up to 2 months, starting from the day the control tumors were rejected (Figure 7C). Of interest, implanted CD8<sup>-/-</sup> mice reproduced the same graft survival curve obtained by the wild-type C57Bl/6 strain, indicating that CD8 T cells are not implicated in the rejection of xenogenic cells. In contrast, NK deficiency is permissive to xenografting since 80% of *beige* mice accepted the transplant for a period longer than 100 days after transplantation (Figure 7C). In addition, the rejection profile was faster in CD4<sup>-/-</sup> mice when compared with wild-type or CD8<sup>-/-</sup> mice, implying that CD4 lymphocytes are necessary for GIFT15-mediated graft tolerance (Figure 7C).

**Discussion**

We have previously demonstrated that the merging of 2 distinct immune-stimulatory cytokines—GM-CSF and IL-2—can lead to a fusokine with synergistic proinflammatory properties in the setting of cancer immunotherapy.<sup>4</sup> Operating within the same developmental mind frame, we sought to improve this antitumor biopharmaceutical by generating a GM-CSF and IL-15 fusokine (aka, GIFT15). We observed that B16 melanoma cells expressing GIFT15 displayed markedly enhanced tumor growth properties in vivo. This observation was contradictory to what our working hypothesis had predicted. In an attempt to decipher this totally unexpected result, we first observed that tumor-associated angiogenesis was markedly

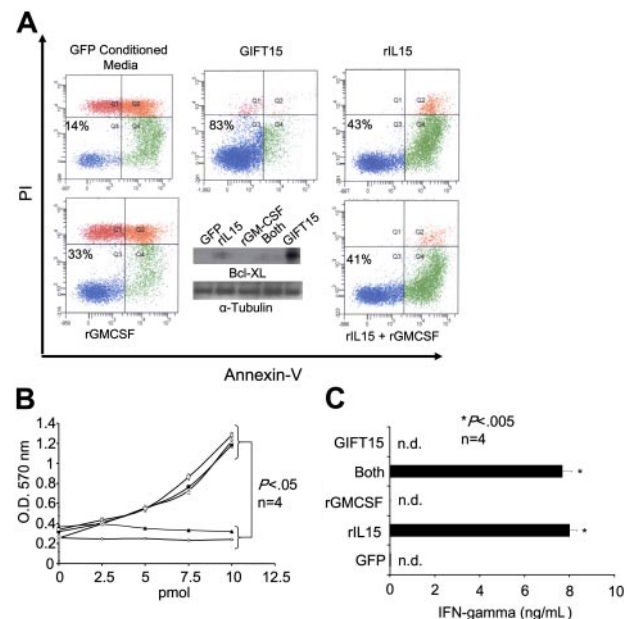


**Figure 5. GIFT15 and biochemical responses.** (A) GIFT15 and splenocyte apoptosis. Splenocytes cultured for 36 hours in the presence of equimolar concentrations of cytokines were stained for PI and annexin-V. The same conditions were applied for Bcl-XL immunoblotting.  $\alpha$ -Tubulin was used as loading control for this experiment. (B) Splenocyte proliferation. Splenocytes ( $10^5$ ) were cultured with increasing concentrations of cytokines for 72 hours before MTT incorporation. Results are shown as mean of triplicates  $\pm$  SEM of 1 representative experiment of 2 independent assays ( $P < .05$  between rIL-15 [■], rIL-15 + rGM-CSF [X], GIFT15 [□], and rGM-CSF [▲], or GFP CM [◇]). (C) Splenocyte activation and secretion of IFN- $\gamma$ . The supernatant of  $10^5$  splenocytes cultured for 36 hours in the presence of GFP CM inoculated with cytokines or GIFT15 CM was used to detect the presence of IFN- $\gamma$  by ELISA. Results are shown as mean of quadruplicate  $\pm$  SED of 1 representative experiment of 5 (nd = not detected;  $P < .005$  between rIL-15 or rIL-15 + rGM-CSF and GFP control group).

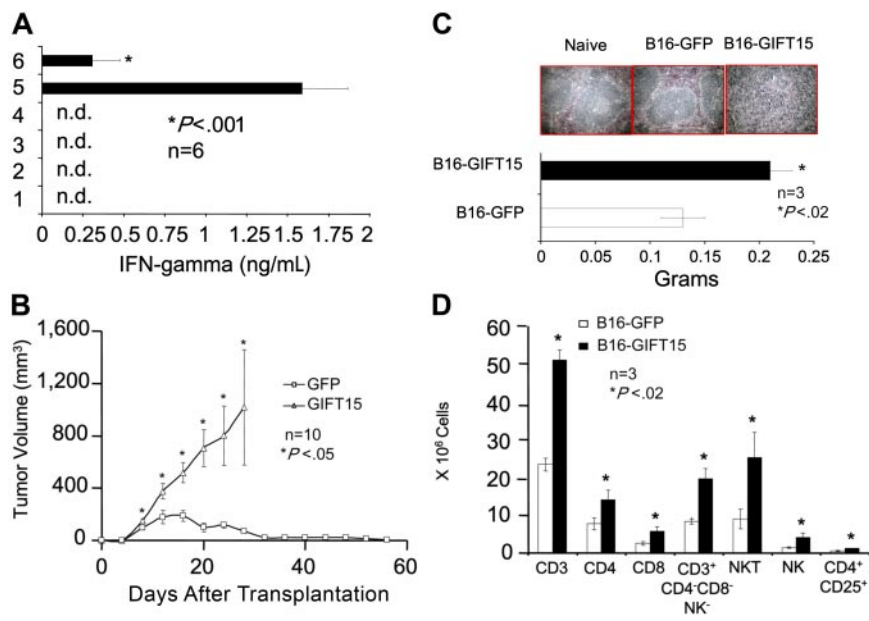


**Figure 6. GIFT15 and allogeneic tumor transplantation.** (A) GIFT15 direct effect on the 2-way MLR. Purified GIFT15 (0.18 pmol) was added directly to  $1.5 \times 10^5$  BALB/c +  $1.5 \times 10^5$  C57BL/6 splenocytes for 72 hours. The supernatant was tested by ELISA for IFN- $\gamma$ . Every condition was performed in six replicates  $\pm$  SED ( $P < .001$  between MLR condition containing GIFT15 and BALB/c + C57BL/6 only). (B) Effect of GIFT15 on B16F0 tumor growth in allogeneic BALB/c mice. Live B16-GFP or GIFT15 cells ( $10^7$ ) were transplanted subcutaneously in immunocompetent BALB/c mice ( $n = 10$ ), and tumor volume was monitored over time. The GIFT15 experiment had to be stopped by day 28 after transplantation due to large tumors developed by these mice ( $P < .05$  between B16-GIFT15 and GFP group). Results are shown as mean tumor volume  $\pm$  SED. (C) GIFT15 BALB/c mice developed splenomegaly. Splenomegaly was observed in mice that had received a transplant of a GIFT15 tumor, based on the spleen's weight characterized by white pulp structural loss as shown by H&E staining. Splens from naive or B16-GFP mice were used for comparison. Results are shown as mean  $\pm$  SED. (D) Increased T- and NK-cell number within the GIFT15 group. Flow cytometry analysis performed on splenocytes from GIFT15 or GFP mice revealed a significant increase in the absolute number of T and NK cells ( $n = 3$ ;  $P < .02$  between the GIFT15 and GFP group). Results are shown as mean average of triplicate  $\pm$  SED.

enhanced in association with a robust recruitment of TAMs, and we further noted that tumor-associated lymphoid cells, in particular NK/NKT cells, were significantly reduced in number. These 2 seminal observations led us to revise our hypothesis on the putative biochemical effect of GIFT15: GIFT15 behaves as a proangiogenic and immunosuppressive compound. These interesting and unantici-

pated properties suggest that GIFT15 may be useful as a compound for treatment of those medical ailments in which pharmaceutical immunosuppression and/or angiogenesis are desirable. To best understand the cellular physiology and biochemistry of GIFT15, we chose to tackle the investigation of angiogenesis and immunosuppression distinctly.

Our initial observation that B16-GIFT15 cells led to massive recruitment of TAMs gave us the insight that host-derived macrophages may be playing a significant role in the observed enhanced angiogenesis. It has been previously shown that GM-CSF and IL-15 can induce migration of macrophages both in vitro and in vivo.<sup>4,7</sup> Since macrophages express both the GM-CSFR and the IL-15R, it follows that GIFT15 would lead to selective recruitment of these cells. Not surprisingly, we found GIFT15 to be a potent chemotactic agent for macrophages in vitro. There is much precedent in the field of cancer angiogenesis of TAMs playing an important role in releasing a wide array of proangiogenic factors as part of a maladaptive injury repair response to a "wound that does not heal."<sup>14-16</sup> We demonstrate that primary peritoneal macrophages stimulated with GIFT15 protein preferentially phosphorylate STAT3 via the IL-2/IL-15  $\beta$  chain and subsequently adopt an unprecedented phenotype where they secrete TIMP-2 de novo. Indeed, there is virtually no published precedent describing TIMP-2 production by monocyte/macrophages, suggesting a completely novel property of macrophages. TIMP-2 is known to act either as an inhibitor of MMP-2 if a soluble complex is formed or as an activator if it is bound to MT1-MMP on cell surfaces, which can lead to matrix remodeling and angiogenesis.<sup>17,18</sup> Moreover, STAT3 phosphorylation has been shown to control the level of MMP-2 secretion by directly binding to its promoter and activating gene expression,<sup>30</sup> suggesting that both TIMP-2 and STAT3 hyperphosphorylation can lead to MMP2 secretion and activation. Indeed, enzymatically active MMP-2 was found to be produced by GIFT15-treated macrophages. MMP-2 possesses a variety of functions, such as anti-inflammation, increasing the levels of active TGF- $\beta$ , as well as the activation of VEGF and of other growth factors.<sup>31-37</sup> In fact, significantly increased levels of active TGF- $\beta$  and VEGF levels were documented in GIFT15-treated macrophages. Although the qualitative interaction of GIFT15 with the

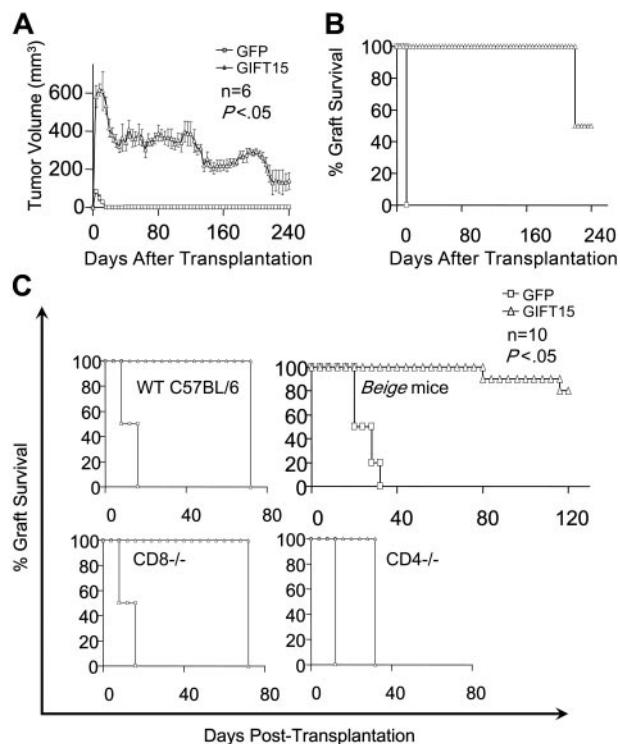


**Figure 7. GIFT15 and tumor xenotransplantation.** (A-B) GIFT15 effect on U87GM xenotransplantation. Immunocompetent BALB/c mice ( $n = 6$ ) were grafted with  $10^7$  live U87-GFP ( $\square$ ) or GIFT15 ( $\triangle$ ) subcutaneously, and tumor volume as well as percentage survival were monitored over 8 months ( $P < .05$  between the GIFT15 and GFP group). (C) Xenotransplantation of U87-GFP/GIFT15 in WT C57BL/6 or KO mice. Live U87-GFP or GIFT15 cells ( $10^7$ ) were transplanted subcutaneously in WT C57BL/6 ( $n = 6$ /group), CD8 $^{-/-}$  ( $n = 10$ /group), CD4 $^{-/-}$  ( $n = 10$ /group), or beige ( $n = 10$ /group) mice, and graft survival was monitored over time ( $P < .05$  between U87-GIFT15 and GFP). Results are shown as mean tumor volume  $\pm$  SED.

GMCSFR appears identical to that of monomeric GMCSF, it must be noted that GMCSF's half-life *in vivo* is more than 240 minutes,<sup>38,39</sup> whereas IL-15 has a much shorter plasma half-life of less than 1 minute.<sup>40</sup> Therefore, it is possible that the *in vivo* half-life of GIFT15 is closer to that of native GMCSF and may lead to prolonged interaction with the IL-15R. In sum, GIFT15 appears to act as a chemotactic agent for macrophages *in vivo* and also modulates their phenotype in a manner rendering them profoundly proangiogenic.

A second seminal observation is the extensive cell-mediated immune suppression by GIFT15 that tolerizes to both allogeneic and xenogenic somatic cell implantation in otherwise immunologically intact recipient mice. On a molecular basis, we have found that GIFT15 has increased affinity for the IL-15R  $\alpha$  chain and also leads to asymmetrical signaling through the IL-15R complex manifest as STAT3 hyperphosphorylation and reciprocal STAT5 underphosphorylation in lymphoid cells. Downstream effects of STAT3/STAT5 asymmetrical signaling include induction of Bcl-XL and suppression of IFN- $\gamma$  production leading to protection from apoptosis and anergy, respectively. The latter observation is of particular interest since it suggests that GIFT15 can quite literally shut down IFN- $\gamma$  production in "activated" lymphoid cells. Indeed, we found that GIFT15 could significantly antagonize IFN- $\gamma$  secretion arising from a 2-way MLR. Since STAT3 activation has recently been reported to mediate immunosuppression by inhibiting the expression of proinflammatory cytokines,<sup>25,26</sup> we propose that the combined effect of enhanced STAT3 activation coupled to a relative decrease in STAT5 phosphorylation may explain the potent blunting of the IFN- $\gamma$  response following GIFT15 exposure.

The B16 melanoma cell line is syngeneic to C57Bl/6 mice, and will lead to tumor growth when implanted subcutaneously in immune-competent C57Bl/6 mice. Indeed, B16 tumors fail to induce an effective immune response in immunologically naive C57Bl/6 mice and are incapable of generating tumors in MHC-mismatched BALB/c mice. In light of the remarkable immunosuppressive effects of GIFT15, we tested whether its expression could protect allogeneic tumor cells from rejection in immune-competent MHC-mismatched recipient animals. As proof of concept, B16-GIFT15 (H-2K<sup>b</sup>) cells were grafted in MHC-mismatched BALB/c (H-2K<sup>d</sup>) mice, and we observed that tumors secreting GIFT15 were accepted in all recipient mice, while controls were tumor free. We observed that B16 tumor cells are associated with a CD3<sup>+</sup> lymphoid cell infiltrate and that the composition of this infiltrate is characterized by depletion of NK/NKT cells in the presence of GIFT15. Since tumor growth is accelerated in this setting, it suggests that NK/NKT cells may play a role in delaying syngeneic tumor growth in immunologically naive mice. We further investigated the utility of GIFT15 immunosuppression in the context of xenotransplantation. In this case, a transduced polyclonal population of the human glioma cell line U87GM was transplanted subcutaneously in BALB/c mice. All mice accepted the GIFT15 xenograft for up to 7 months, whereas the control U87-GFP xenograft was rejected 12 days after injection. Since different mouse strains generate variable immune responses,<sup>41</sup> we pursued our studies by performing xenotransplantation on C57Bl/6 mice, which are known to possess a biased Th1 immune response.<sup>42</sup> Even though both control and GIFT15-expressing xenografts were rejected in these mice, there was a 2-month delay for the complete regression of the U87-GIFT15 transplants in comparison with the U87-GFP group.

In contrast, in the allogeneic tumor implant model, xenogenic human tumor cells cannot lead to a physiological immune synapse

in murine hosts due to the interspecies discrepancy between human MHC and murine TCR, thereby limiting cellular rejection to MHC-independent cytotoxic cells such as NK. Indeed, NK cells appear to be important effectors in xenotissue rejection.<sup>43</sup> Our model system behaves similarly, since we observed that NK-deficient mice are permissive to human xenograft tumor growth and that CD4<sup>-/-</sup> and CD8<sup>-/-</sup> mice robustly reject xenografts. The observation that GIFT15 allows human xenograft tumor growth in normal mice strongly supports the hypothesis that its suppressive effect—in the xenogenic setting—is targeted toward NK cells. Furthermore, this anti-NK effect of GIFT15 is dependent upon interplay with CD4 cells. We speculate that GIFT15 modulates a subset of CD4 cells that may interact with NK directly. Therefore, in the absence of a species-paired immunologic synapse between effector and target cell, GIFT15 likely tolerizes to xenografts by promoting a suppressive cross talk between host-derived CD4 and NK cells.<sup>44</sup>

Taken together, our observations and experiments support the hypothesis that GIFT15 possesses novel biochemical properties leading to altered affinities to components of the IL-15R and asymmetrical downstream signaling via its 2 dependent STAT/JAK pathways in lymphomyeloid cells. As a result, cellular proliferation, reduced apoptosis, and blunting of the IFN- $\gamma$  response following activation can be achieved in lymphoid cells as well as a proangiogenic response by macrophages. The sum of these effects mediates a profound immunosuppressive state permissive to allo/xenotransplantation that is CD4 dependent. Considering these biochemical properties, we speculate that the GIFT15 fusion protein can be exploited using 2 different approaches: tissue transplantation and autoimmune disease. First, genetic modification of allogeneic or xenogenic somatic cells or tissue to express GIFT15 can be readily achieved using currently available gene transfer technology and *in vivo* tolerance achieved as we have here demonstrated. As a specific and achievable translational example, we could envisage GIFT15 engineering of islet cells from allogeneic human or xenogenic nonsimian source and using these cells for the treatment of type I diabetes without need of systemic immunosuppressive regimen in the recipient. Indeed, a wide array of cells/tissues/organs from allogeneic or xenogenic sources could be similarly engineered for treatment of a variety of human ailments. Another therapeutic avenue for this fusokine could be its use as a purified recombinant protein that can be administered parenterally for the treatment of severe, life-threatening or debilitating autoimmune diseases such as graft-versus-host disease or multiple sclerosis where immunosuppression is clinically desirable. In conclusion, we have generated a novel biopharmaceutical providing a potential therapeutic platform for tolerization to immunologically mismatched tissue and treatment of ailments responsive to pharmacological immunosuppression.

---

## Acknowledgments

This study was supported by a Canadian Institute for Health Research (CIHR) operating grant (MOP-15017). Sheldon Biotechnology Centre at McGill University is supported by a Multi-User Maintenance Grant from CIHR. M.R. is a recipient of a Fonds de recherches en Santé du Québec (FRSQ) Scholarship, and J.G. is an FRSQ chercheur boursier sénior.

We thank Dr M. Hancock (Sheldon Biotechnology Center)

for the BIAcore experiments. We thank Drs N. Eliopoulos, I. Copland, and J. Stagg for technical advice and materials.

## Authorship

Contribution: M.R. designed research, performed research, analyzed data, and wrote the paper; J.H.W. designed and performed

research; B.A., L.L., and M.F. performed research; and J.G. designed research, analyzed data, and wrote the paper.

Conflict of interest disclosure: The authors declare no competing financial interests.

Correspondence: Jacques Galipeau, Jewish General Hospital, 3755 Cote Ste-Catherine Road, Montreal, QC, Canada, H3T1E2; e-mail: jacques.galipeau@mcgill.ca.

## References

1. Dranoff G, Jaffee E, Lazenby A, et al. Vaccination with irradiated tumor cells engineered to secrete murine granulocyte-macrophage colony-stimulating factor stimulates potent, specific, and long-lasting anti-tumor immunity. *Exp Hematol*. 1993; 90:3539-3543.
2. Irvine KR, Rao JB, Rosenberg SA, Restifo NP. Cytokine enhancement of DNA immunization leads to effective treatment of established pulmonary metastases. *J Immunol*. 1996;156:238-245.
3. Gillies SD, Lan Y, Brunkhorst B, Wong WK, Li Y, Lo KM. Bi-functional cytokine fusion proteins for gene therapy and antibody-targeted treatment of cancer. *Cancer Immunol Immunother*. 2002;51: 449-460.
4. Stagg J, Wu JH, Bougamin N, Galipeau J. Granulocyte-macrophage colony stimulating factor and interleukin-2 fusion cDNA for cancer gene therapy. *Cancer Res*. 2004;64:8795-8799.
5. Waldmann TA, Tagaya Y. The multifaceted regulation of interleukin-15 expression and the role of this cytokine in NK cell differentiation and host response to intracellular pathogens. *Annu Rev Immunol*. 1999;17:19-49.
6. Tagaya Y, Bamford RN, DeFilippis AP, Waldmann TA. IL-15: a pleiotropic cytokine with diverse receptor/signaling pathways whose expression is controlled at multiple levels. *Immunity*. 1996;4:329-336.
7. Fehniger TA, Caligiuri MA. Interleukin 15: biology and relevance to human diseases. *Blood*. 2001; 97:14-32.
8. Pulendran B, Dillon S, Joseph C, Curiel T, Banachereau J, Mohamadzeadeh M. Dendritic cells generated in the presence of GM-CSF plus IL-15 prime potent CD8+ Tc1 responses in vivo. *Eur J Immunol*. 2004;34:66-73.
9. Perri SR, Nalbantoglu J, Annabi B, et al. Plasminogen kringle 5-engineered glioma cells block migration of tumor-associated macrophages and suppress tumor vascularization and progression. *Cancer Res*. 2005;65:8359-8365.
10. Mrozek E, Anderson P, Caligiuri M-A. Role of interleukin-15 in the development of CD56+ natural killer cells from CD34+ hematopoietic progenitor cells. *Blood*. 1996;87:2632-2640.
11. Ohteki T, Yoshida H, Matsuyama, et al. The transcription factor interferon regulatory factor 1 (IRF-1) is important during the maturation of natural killer 1.1+ T-cell receptor-alpha/beta+ (NK1+T) cells, natural killer cells, and intestinal intraepithelial T cells. *J Exp Med*. 1998;187:967-972.
12. Fehniger TA, Shah MH, Turner MJ, et al. Differential cytokine and chemokine gene expression by human NK cells following activation with IL-18 or IL-15 in combination with IL-12: implications for the innate immune response. *J Immunol*. 1999; 162:4511-4520.
13. Atedzoe BN, Ahmand A, Menezes J. Enhancement of natural killer cell cytotoxicity by the human herpes-7 via IL-15 induction. *J Immunol*. 1997;159:4966-4972.
14. Nesbit M, Schaidler H, Miller TH, Herlyn M. Low-level monocyte chemoattractant protein-1 stimulation of monocytes leads to tumor formation in nontumorigenic melanoma cells. *J Immunol*. 2001;166:6483-6490.
15. Sica A, Sacconi A, Bottazzi B, et al. Autocrine production of IL-10 mediates defective IL-12 production and NF-kB activation in tumor-associated macrophages. *J Immunol*. 2000;164:762-767.
16. Dinapoli MR, Calderon CL, Lopez DM. The altered tumoricidal capacity of macrophages isolated from tumor-bearing mice is related to reduced expression of the inducible nitric oxide synthase gene. *J Exp Med*. 1996;183:1323-1329.
17. Egblad M, Werb Z. New functions for the matrix metalloproteinases in cancer progression. *Nat Rev*. 2002;2:161-174.
18. Itoh T, Tanioka M, Yoshida H, Yoshioka T, Nishimoto H, Itoharu S. Reduced angiogenesis and tumor progression in gelatinase A-deficient mice. *Cancer Res*. 1998;58:1048-1051.
19. Xie TX, Huang FJ, Aldape KD, et al. Activation of stat3 in human melanoma promotes brain metastasis. *Cancer Res*. 2006; 66:3188-3196.
20. Lorenzen I, Dingley AJ, Jacques Y, Grotzinger J. The structure of the interleukin-15alpha receptor and its implications for ligand binding. *J Biol Chem*. 2006;281:6642-6647.
21. Bernard J, Harb C, Mortier E, et al. Identification of an interleukin-15alpha receptor-binding site on human interleukin-15. *J Biol Chem*. 2004;279: 24313-24322.
22. Stauber DJ, Debler EW, Horton PA, Smith KA, Wilson IA. Crystal structure of the IL-2 signaling complex: paradigm for a heterotrimeric cytokine receptor. *Proc Natl Acad Sci U S A*. 2006;103: 2788-2793.
23. Catlett-Falcone R, Landowski TH, Oshiro MM, et al. Constitutive activation of STAT3 signaling confers resistance to apoptosis in human U266 myeloma cells. *Immunity*. 1999;10:105-115.
24. Niu G, Bowman T, Huang M, et al. Roles of activated Src and STAT3 signaling in melanoma tumor cell growth. *Oncogene*. 2002;21:7001-7010.
25. Wang T, Niu G, Kortylewski M, et al. Regulation of the innate and adaptive immune responses by Stat-3 signaling in tumor cells. *Nat Med*. 2003;10: 48-54.
26. Kortylewski M, Kujawski M, Wang T, et al. Inhibiting Stat3 signaling in the hematopoietic system elicits multicomponent antitumor immunity. *Nat Med*. 2005;11:1314-1321.
27. Kisselva T, Bhattacharya S, Braunstein J, Schindler C-W. Signaling through the JAK/STAT pathway, recent advances and future challenges. *Gene*. 2002;285:1-24.
28. Bromberg J, Darnell JE. The role of STATs in transcriptional control and their impact on cellular function. *Oncogene*. 2000;19:2468-2473.
29. Smithgall TE, Briggs SD, Schreiner S, Lerner EC, Cheng H, Wilson MB. Control of myeloid differentiation and survival by Stats. *Oncogene*. 2000;19: 2612-2618.
30. Xie TX, Wei D, Liu M, et al. Stat3 activation regulates the expression of matrix metalloproteinase-2 and tumor invasion and metastasis. *Oncogene*. 2004;23:3550-3560.
31. Fukai F, Ohtaki M, Fujii N, et al. Release of biological activities from quiescent fibronectin by a conformational change and limited proteolysis by matrix metalloproteinases. *Biochemistry*. 1995; 34:11453-11459.
32. Fowlkes JL, Enghild JJ, Suzuki K, Nagase H. Matrix metalloproteinases degrade insulin-like growth factor-binding protein-3 in dermal fibroblast cultures. *J Biol Chem*. 1994;269:25742-25746.
33. Hashimoto G, Inoki I, Fujii Y, Aoki T, Ikeda E, Okada Y. Matrix metalloproteinases cleave connective tissue growth factor and reactivate angiogenic activity of vascular endothelial growth factor 165. *J Biol Chem*. 2002;277:36288-36295.
34. Ito A, Mukaiyama A, Itoh Y, et al. Degradation of interleukin 1β by matrix metalloproteinases. *J Biol Chem*. 1996;271:14657-14660.
35. McQuibban GA, Gong JH, Tam EM, McCulloch CA, Clark-Lewis I, Overall CM. Inflammation dampened by gelatinase A cleavage of monocyte chemoattractant protein-3. *Science*. 2000;289: 1202-1206.
36. McQuibban GA, Gong JH, Wong JP, Wallace JL, Clark-Lewis I, Overall CM. Matrix metalloproteinase processing of monocyte chemoattractant proteins generates CC chemokine receptor antagonists with anti-inflammatory properties in vivo. *Blood*. 2002;100:1160-1167.
37. Imai K, Hiramatsu A, Fukushima D, Pierschbacher MD, Okada Y. Degradation of decorin by matrix metalloproteinases: identification of the cleavage sites, kinetic analyses and transforming growth factor-beta1 release. *Biochem J*. 1997; 322:809-814.
38. Sainathan SK, Tu L, Bishnupuri KS, et al. PEGylated murine granulocyte-macrophage colony-stimulating factor: production, purification, and characterization. *Protein Expr Purif*. 2005;44:94-103.
39. Burgess AW, Metcalf D. Serum half-life and organ distribution of radiolabeled colony stimulating factor in mice. *Exp Hematol*. 1977;5:456-464.
40. Pettit DK, Bonner TP, Eisenman J, et al. Structure-function studies of interleukin-15 using site-specific mutagenesis, polyethylene glycol conjugation, and homology modeling. *J Biol Chem*. 1997;272:2312-2318.
41. Mosmann TR, Coffman RL. Heterogeneity of cytokine secretion patterns and functions of helper T cells. *Adv Immunol*. 1989;46:111-147.
42. Ulett GC, Ketheesan N, Hirst RG. Cytokine gene expression in innately susceptible BALB/c mice and relatively resistant C57Bl/6 mice during infection with virulent *Burkholderia pseudomallei*. *Infect Immun*. 2000;68:2034-2042.
43. Kitchens WH, Uehara S, Chase CM, Colvin RB, Russell PS, Madsen JC. The changing role of natural killer cells in solid organ rejection and tolerance. *Transplantation*. 2006;81:811-817.
44. Wahl SM, Wen J, Moutsopoulos NM. The kiss of death: interrupted by NK-cell close encounters of another kind. *Trends Immunol*. 2006;4:161-164.